Paper No.
7038

NACE INTERNATIONAL CORROSION 2016 CONFERENCE & EXPO

Corrosion of Metals in Treated Wood Examined by Synchrotron Based XANES and XFM

Samuel L. Zelinka, Joseph E. Jakes, Grant T. Kirker, and Leandro Passarini
US Forest Service, Forest Products Laboratory
1 Gifford Pinchot Dr.
Madison, WI 53726
USA

Barry Lai
Argonne National Laboratory
9700 S. Cass Ave.
Argonne, IL 60439
USA

ABSTRACT

Copper based waterborne wood preservatives are frequently used to extend the service life of wood products used in outdoor environments. While these copper based treatments protect the wood from fungal decay and insect attack, they increase the corrosion of metals embedded or in contact with the treated wood. Over the past ten years, several studies have looked at the corrosion mechanisms for metals in contact with copper treated wood. These studies have concluded that the most plausible corrosion mechanism involves the migration of copper ions from the wood treatment through the wood to the metal surface, where they are then reduced. Despite the evidence for this corrosion mechanism, copper is usually not detected in corrosion products as the proposed mechanism would suggest.

Here, we examine wood that was in contact with corroding metal using synchrotron based X-ray fluorescence microscopy (XFM) and X-ray Absorption Near Edge Spectroscopy (XANES) to test whether the previously proposed corrosion mechanism is correct and if so, why copper is not deposited on the metal surface. With XFM we are able to detect copper in the wood and construct a copper concentration profile map with a spatial resolution of 0.5µm down to trace (less than 0.01 µg cm^{-2}) concentrations. We compliment these measurements with XANES, a technique that allows us to differentiate between the different ionic states of copper in the wood. These measurements give, for the first time, an experimental method to test the previous theories of the role of copper in the corrosion metals in treated wood.

Key words: preservative treated wood, steel, cupric ions

INTRODUCTION

The corrosion of metals embedded in wood has been extensively studied over the past 10 years. When wood is used in environments with excessive moisture, it is frequently treated with wood preservatives, chemicals that protect the wood from attack from insects and fungi. In 2004, there was a voluntary wood preservative regulation change in the United States, which restricted the use of chromated copper arsenate (CCA), the most common wood preservative for the previous 50 years.[1] Several wood preservatives replaced CCA in the marketplace. These wood preservatives contained higher amounts of copper than CCA, and shortly after they were introduced to the market, corrosion became a major concern.[2] Corrosion research has focused on understanding the mechanism of corrosion in preservative treated wood and also understanding how chemical differences between preservatives affect their corrosiveness.

One obvious reason for the corrosiveness of wood preservatives is that they are primarily comprised of copper, believed to be in the form of cupric ions which are thermodynamically unstable in the presence of steel and hot-dip galvanized steel fasteners. Zelinka et al. proposed that the corrosion mechanism for metals in copper treated wood involved the reduction of cupric ions in the wood as the cathodic reaction.[3] The corrosion mechanism involves two steps: diffusion of cupric ions from the wood to the metal surface and an electron transfer reaction at the metal surface. The proposed mechanism was based upon three experimental observations. Firstly, the Pourbaix diagram of copper shows that open circuit potentials of steel and zinc galvanized fasteners fall in a region where copper metal is the stable phase.[4] Secondly, the corrosion rate of steel and zinc galvanized fasteners increases with increasing copper concentration in the wood.[5, 6] Thirdly, differences in the corrosiveness of commercial wood preservatives can be explained almost entirely by differences in the pH and copper concentration of water extracted from the wood.[3] Despite evidence that reduction of cupric ions is the primary cathodic reaction, in general, copper has not been detected in the corrosion products collected from steel and hot dip zinc galvanized fasteners when inspected by powder X-ray diffraction (XRD) or energy dispersive X-ray spectroscopy (EDS).[4, 7]

Given the current observations of how copper affects the corrosion of embedded metals but does not appear in the corrosion products, there are several possibilities. The first possibility is that copper ions are reduced, but they remain in the wood and are therefore not found in the corrosion products. In this case, we would expect the copper in the wood near the fastener to have a different oxidation state than copper far from the fastener surface. A second possibility is that the copper ions are reduced near the metal surface but this reduced copper does adhere to the fastener surface and was therefore undetectable in the previous corrosion product analyses. Finally, it is also possible that the corrosion of embedded metals does not involve the reduction of copper.

X-ray fluorescence microscopy (XFM) and X-ray Absorption Near Edge Spectroscopy (XANES) are well suited for examining and understanding the role of copper in the corrosion of metals in treated wood. In XFM, a monochromatized X-ray beam whose energy is above the absorption edge of the elements of interest is raster scanned over the sample; the resulting fluorescent photons can be used to map the elements present and their concentration.[8-10] In wood, XFM has been used to examine the infiltration of Br-labeled adhesives into the wood cell wall as well as diffusion of ions (including copper) through the wood cell wall.[11, 12] In XANES, a tunable monochromatized X-ray beam is scanned from just below to slightly over the absorption edge; the fluorescence intensity as a function of energy depends upon the element coordination and oxidation state.[13-17]

In this study we utilize XFM and XANES to examine the role of copper in the corrosion mechanism of treated wood. The copper micro-distribution and oxidation states near the fastener surface were examined on samples that came from previous laboratory experiments on the corrosion of metals in treated wood.[7]

EXPERIMENTAL PROCEDURE

The wood samples were saved from a previous laboratory exposure test of the corrosion of fasteners in preservative treated wood.[7] Steel fasteners were driven into 50 mm by 38 mm by 90 mm blocks of southern pine (*Pinus spp.*) and the wood-metal assembly was placed above liquid water in a desiccator for one year. The relative humidity in the desiccator was fixed at 100% by the Gibbs Phase Rule. The average wood moisture content ($g_{water}/g_{dry\ wood}$) was 24.6%.

The four different wood preservative treatments examined were chromated copper arsenate (CCA), alkaline copper quaternary carbonate (ACQ), micronized copper quanternary (MCQ), and copper azole (CuAz). CCA, ACQ, and CuAz are standardized by the American Wood Protection Association standard P5.[18] MCQ is established and regulated by an ICC-ES evaluation report.[19] The compositions and copper retentions of the preservatives are listed in Table 1. It is important to note that although in some cases the copper is listed as "copper oxide" in the tables, this is used as a convention to set the weight ratio in the AWPA P5 standard; preservative manufacturers are allowed to use a different copper compound so long as the amount of copper is equivalent to the specified ratios. In contrast to ACQ, where the copper is solubilized in a solution of ethanolamine and injected into the wood, MCQ is produced by grinding the copper compounds (usually copper carbonate) into submicron particles and suspending them in solution prior to injection.

Table 1
Preservative compositions and treatment retentions for the wood preservatives examined in this study.

	Composition	Preservative Retention (kg of preservative per m^3 of wood)[a]	Bulk copper concentration (g of copper per m^3 of wood)
CCA Chromated Copper Arsenate (type C)	47.5 wt% CrO3 18.5 wt% CuO 34.0 wt% As2O5	1.6	236
ACQ Alkaline Copper Quaternary (type D)	66.7 wt% CuO 33.3% DDAC[b]	2.9	1529
CuAz Copper Azole (type C)	96.1% Cu 1.95 wt% Tebuconazole 1.95 wt% Propiconazole	0.7	541
MCQ Micronized Copper Quaternary	66.7 wt% CuO 33.3% DDAC	5.0	2636

[a]Actual retention in bulk wood as determined by Inductively coupled plasma atomic emission spectroscopy (ICP-AES) in previous work [7]
[b]DDAC, didecyldimethylammonium carbonate

After the exposure test, the fasteners were removed by cutting the wood around the fastener. The wood sections next to the fastener were stored under climate controlled (office) conditions for several years until this study. To prepare the wood samples for XFM and XANES, two µm–thick transverse sections were prepared using a diamond knife fit into an Ultramicrotome. Sections were cut under ambient temperature and dry. The sections were secured between two 200 nm–thick low stress silicon nitride windows for the experiments.

The XFM and XANES experiments were conducted at beamline 2-ID-D at the Advanced Photon Source at Argonne National Laboratory† (Argonne, IL, USA). For XFM, the incident X-ray beam energy was 9keV. Elemental maps were built in 0.2 µm step sizes and a 5 ms dwell time for each step. Data analysis was carried out by the MAPS† software package where the full spectra were fit to modified Guassian peaks, the background was iteratively calculated and subtracted, and the results were compared to standard reference materials NBS 1832 and 1833.[20] XFM maps presented in this paper utilized a 3x3 pixel median filter.

Copper XANES scans were collected by scanning over copper K-edge (8980 eV) from 8960eV to 9040eV with a step size of 0.5eV. The beam spot size is about 0.2 µm. The dwell time at each energy depended on the relative signal (amount of copper) and ranged from 2s-10s per energy step. Data were analyzed by first exporting the copper fluorescence signal and the total absorption from MAPS. The ratio of the copper signal to the absorption was then analyzed in ATHENA† (version 0.9.22). Using the software, the data were edge step normalized so that they could be directly compared to other XANES data.[21] In some cases the software was used to "merge" scans from different regions by averaging the normalized absorption at each energy. Merging scans reduces the noise within the XANES scans and allows for easier comparison across different samples.

RESULTS

Representative XFM results are shown in Figures 1 and 2. Figure 1 is an overview map of iron and copper over a section cut from wood treated with ACQ. Figure 2 is a high resolution scan of the same elements for wood treated with CuAz taken close to the side of the specimen that was next to the fastener. Elemental maps for MCQ and CCA showed similar trends to the ACQ and CuAz maps. In both figures, there appears to be a copper depletion zone near the fastener. This copper depletion zone can be more clearly seen in Figure 2 since in Figure 1 the cells with depleted copper can be seen only in the iron map. Interestingly, the copper-depleted zone appears to roughly correspond to the same distance that iron diffused into the cell wall from the corroded fastener. The elemental maps were used to select locations for XANES measurements.

† Trade name.

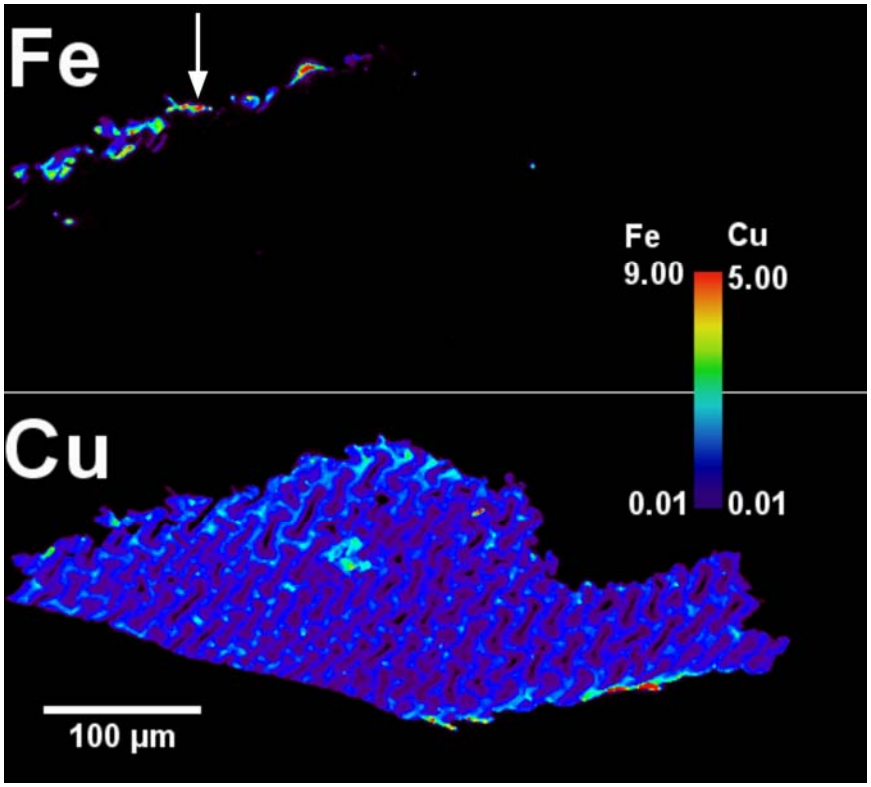

Figure 1: Overview XFM scan for wood treated with ACQ. The arrow indicates the side of the wood section closest to the fastener. The units for the color intensity scale bar are µg cm^{-2}. Note that the cells closest to the fastener can only be seen on the iron map since the copper concentrations are so low.

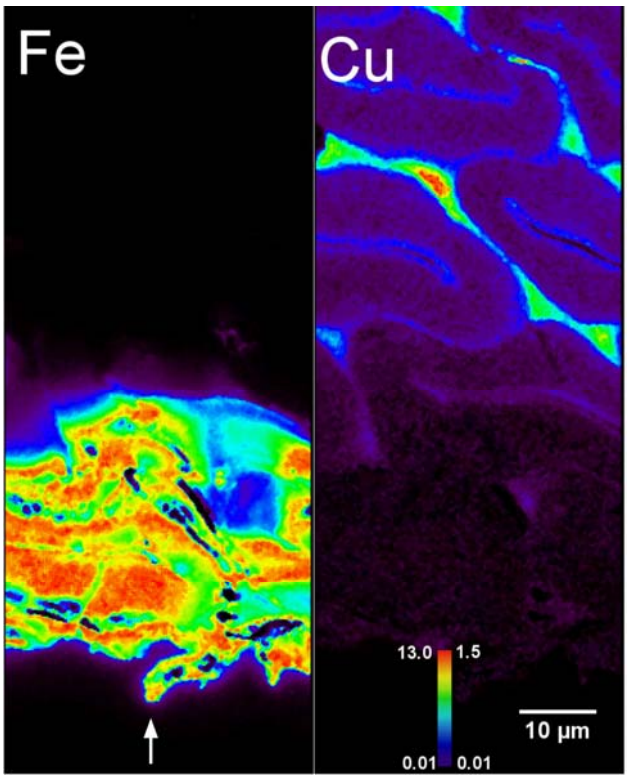

Figure 2: High-resolution XFM scan near the fastener interface for wood treated with CuAz. The arrow indicates the side of the wood section closest to the fastener. The units for the color intensity scale bar are µg cm^{-2}.

XANES measurements were performed in the copper-depleted corrosion affected zone and in the "control" area. These locations were easily distinguishable from the XFM maps. Measurements were taken in both the S2 layer of the secondary cell wall (S2) and the cell corner compound middle lamella (CCCML), as the XFM maps showed that the wood cells had a higher concentration of copper in the middle lamella than in the secondary cell wall layer. Figure 3 shows the XANES spectra taken from the S2 layer (solid line) and middle lamella (dotted line) for each wood treatment taken in the control area. The scans were largely identical between the S2 and CCCML regions; therefore, scans taken from these regions were merged into a single, representative XANES spectra for both the control and corrosion zone.

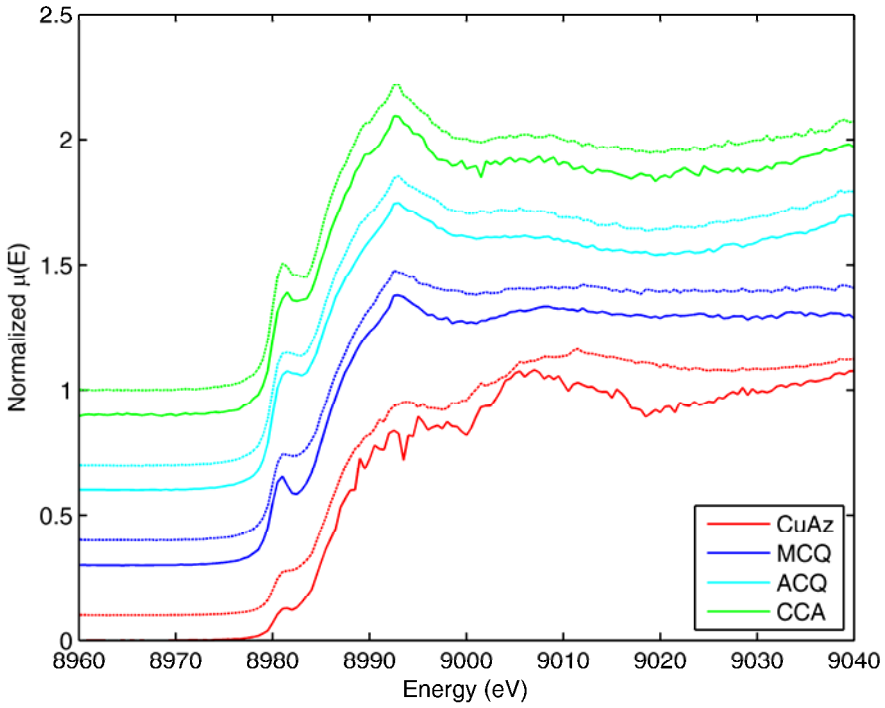

Figure 3: Comparison of the XANES spectra collected in the S2 layer (solid line) and the middle lamella (dotted line) for various wood treatments.

Figure 4 plots the relevant merged XANES data collected in the control regions for the various treatments along with XANES spectra from copper compounds. The XANES spectra from the wood exhibit characteristics of both the cuprous oxide (Cu_2O) and the cupric carbonate ($Cu(CO_3)_2$) spectra. There is a sharp peak at 8982eV that matches the Cu_2O peak and a broad peak between 8990eV and 9000eV that can be seen in the cupric carbonate spectra. It appears that the experimental data are a linear combination of these two spectra. For example, the bold, black curve was created from adding of 70% of the Cu_2O spectra and 30% of the $Cu(CO_3)_2$) spectra at each energy and closely mimics the behavior of treated wood curves.

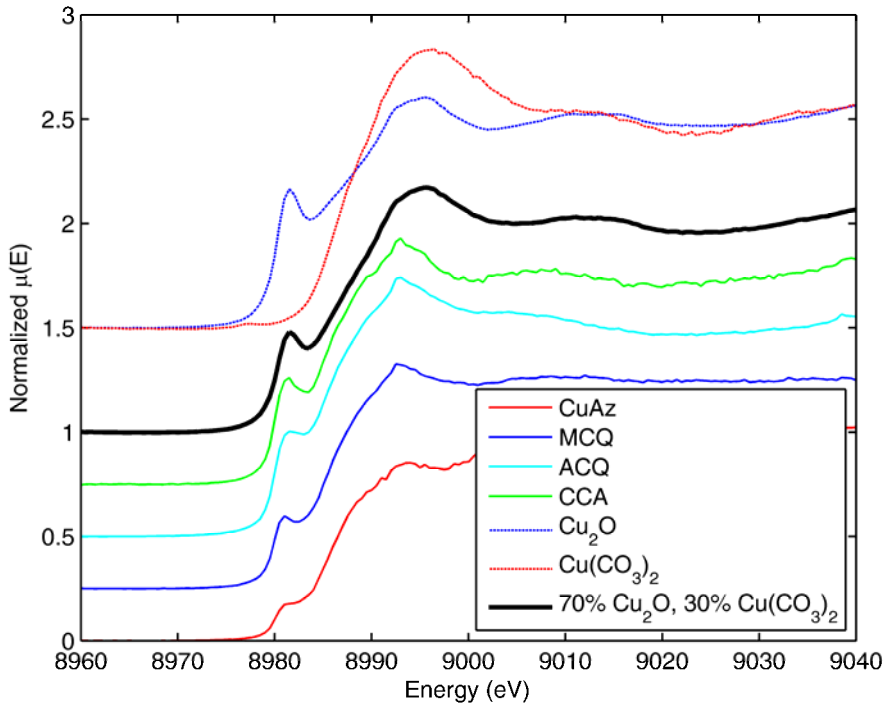

Figure 4: XANES spectra for the various treatments compared against reference materials.

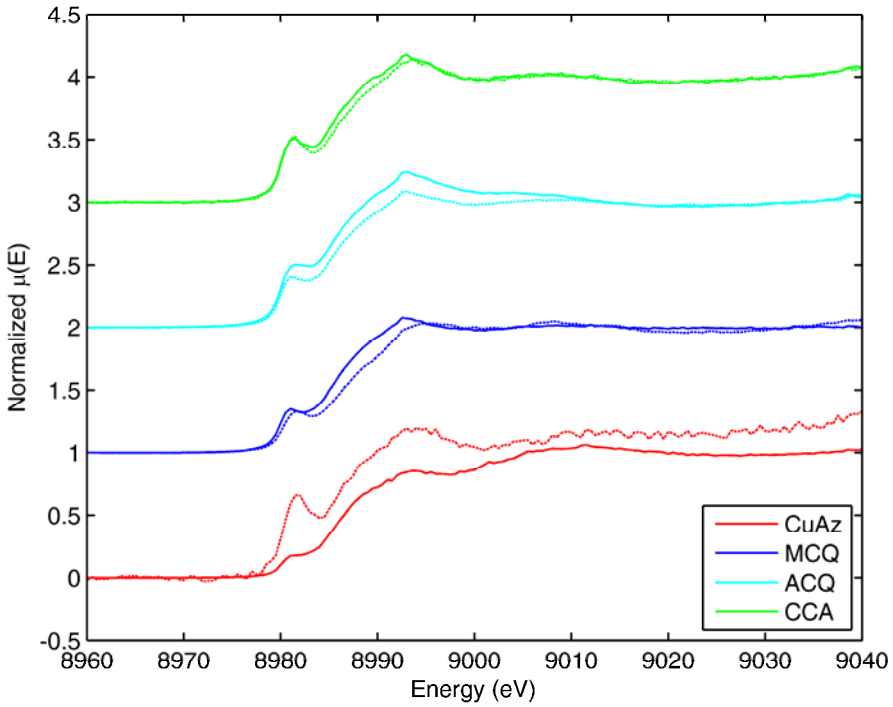

Figure 5: Comparison of the XANES spectra collected in the control zone (solid line) and the corrosion affected zone (dotted line)

In Figure 5, the XANES spectra from control region (solid line) are plotted against the XANES spectra from the corrosion area (dotted line). For the MCQ, ACQ, and CCA treatments, there appear to be no differences in the XANES scans between these two regions, which suggests that the copper oxidation state is the same in both regions. In contrast, for the measurements taken in the CuAz treatment, the XANES spectra appears to be different from the control region, with a much larger peak at 8982eV.

DISCUSSION

The goal of the paper was to better understand the role of copper in the corrosion of metals in wood by using synchrotron based fluorescence microscopy and X-ray absorption near edge spectroscopy. The XFM maps showed a region of copper depletion in wood cells closest to the corroding fastener. XANES data showed that for CCA, MCQ, and ACQ, treatments the oxidation state of copper in the wood remained the same regardless of its proximity to the fastener.

The most exciting result was that there was a zone of copper depletion near the fastener that corresponded with the depth to which iron had diffused into the wood structure. Previously, Zelinka et al. had proposed that the corrosion mechanism in treated wood involved the diffusion of copper from the wood preservative to the metal surface where it was reduced.[3] The depleted copper zones in the XFM data (Figures 1 and 2) support this mechanism. However, in nearly all of the corrosion tests that had been performed, there was no evidence of copper in the corrosion products.[4, 7]

The XFM data also suggested the amount of copper consumed would be too small to detect using energy dispersive X-ray spectroscopy (EDS) or powder XRD. For example, in Figure 2 the copper depletion zone extends 50 µm from the fastener whose radius is 1.5 mm and the average copper concentration in the control and corrosion zones were 0.26 µg cm^{-2} and 0.05 µg cm^{-2}, respectively. If all of the depleted copper were part of the corrosion products, the amount would be approximately 1 ng per 2 µm fastener length or 32 µg for the entire 64 mm long fastener. This extremely small amount of copper produced would likely be undetectable by EDS or a powder XRD examination of the corrosion products. In the future, XFM could be used to examine the corrosion products for the presence of copper to confirm the corrosion mechanism.

While the XFM results give clear evidence of copper migration, the XANES data are equally important in understanding the role of cupric ions in the corrosion mechanism. Except for the CuAz treated wood, the peak positions remained the same in the control zone and the corrosion affected zone. These data show that for most treatments, the oxidation state of copper in the wood is not affected by the corrosion process. Since it is believed that the corrosion mechanism involves the reduction of copper ions from the wood preservative, the XANES data show that this reduction is happening at the fastener surface and not in the wood cell walls.

Interestingly, the XANES spectra for the CuAz treated wood appears to have a different trend from the other 3 wood preservatives and shows some differences between the corrosion affected zone and the control zone. The peak at 8982 eV is much larger in measurements taken in the corrosion affected zone compared to the control zone, but is not shifted along the energy axis. Furthermore, the broad peak between 8990 and 9000 eV is also higher in the corrosion zone but this difference is not as large as it is for the peak at 8982eV. It is unclear why the CuAz treated wood would behave differently than the chemically similar ACQ treated wood. However, it should be noted that these data appear to contain much more noise than any other data set, which suggests that the copper signal may have been especially weak in these measurements. More measurements are needed in the CuAz treated wood to confirm and understand these differences between the XANES spectra of the corrosion affected and control regions.

CONCLUSIONS

This paper used synchrotron based XANES and XFM to examine the role of copper in the corrosion of metals in treated wood. The spatial distribution of the concentration of copper in wood that had been next to corroding fasteners was mapped using XFM. The oxidation state of the copper in the wood immediately next to the fastener and farther away from the fastener was measured using XANES. Together, these data can be used to draw the following conclusions about the role of copper in corrosion mechanism:

- There is a zone near the fastener where there is a much lower concentration of copper. This zone roughly corresponds with the distance that the iron corrosion products have diffused into the wood.
- The oxidation states of the copper in both of these zones remains the same for all treatments, except possibly CuAz.
- The results suggest the corrosion mechanism in treated wood involves copper from the wood preservatives. The mechanism involves the diffusion of copper through the wood to the metal surface where it is reduced.
- Based upon a calculation from the XFM data, the amount of copper consumed in the corrosion reaction would be too small to detect with powder XRD or EDS. This explains why previous examinations of the corrosion of metals in treated wood have failed to detect copper in the corrosion products.

ACKNOWLEDGEMENTS

This work was performed by US Government researchers on official time and is therefore in the public domain and not subject to copyright. Joseph E. Jakes and Samuel L. Zelinka acknowledge funding from the Presidential Early Career Award for Scientists and Engineers (PECASE). The use of Advanced Photon Source facilities was supported by the US Department of Energy, Basic Energy Sciences, Office of Science, under contract number W-31-109-Eng-38.

REFERENCES

1. S. Lebow, "Alternatives to Chromated Copper Arsenate for Residential Construction. Res. Pap. FPL-RP-618", in, U.S.D.A. Forest Service, Forest Products Laboratory, Madison, WI, 2004, pp. 9-9.
2. M. Burkholder, "CCA, NFBA, and the post-frame building industry," Frame Building News 16,5 (2004): p. 6-12.
3. S.L. Zelinka, D.S. Stone, "Corrosion of metals in wood: Comparing the results of a rapid test method with long-term exposure tests across six wood treatments," Corrosion Science 53,5 (2011): p. 1708-1714.
4. S.L. Zelinka, D. Derome, S.V. Glass, "The effect of moisture content on the corrosion of fasteners embedded in wood subjected to alkaline copper quaternary treatment," Corrosion Science 83,1 (2014): p. 67-74.
5. G. Kear, H.-Z. Wu, M.S. Jones, "Weight loss studies of fastener materials corrosion in contact with timbers treated with copper azole and alkaline copper quaternary compounds," Corrosion Science 51,2 (2009): p. 252-262.
6. S.L. Zelinka, D.R. Rammer, "Synthesis of Published and Unpublished Corrosion Data From Long Term Tests of Fasteners Embedded in Wood: Calculation of Corrosion Rates and the Effect of Corrosion on Lateral Joint Strength", in: CORROSION 2011, NACE International, Houston, TX, 2011, pp. Paper No. 11163.

7. S.L. Zelinka, R.J. Sichel, D.S. Stone, "Exposure testing of fasteners in preservative treated wood: gravimetric corrosion rates and corrosion product analyses," Corrosion Science 52,12 (2010): p. 3943-3948.
8. U.E.A. Fittschen, G. Falkenberg, "Trends in environmental science using microscopic X-ray fluorescence," Spectrochimica Acta Part B: Atomic Spectroscopy 66,8 (2011): p. 567-580.
9. T. Paunesku, S. Vogt, J. Maser, B. Lai, G. Woloschak, "X-ray fluorescence microprobe imaging in biology and medicine," Journal of cellular biochemistry 99,6 (2006): p. 1489-1502.
10. B.S. Twining, S.B. Baines, N.S. Fisher, J. Maser, S. Vogt, C. Jacobsen, A. Tovar-Sanchez, S.A. Sañudo-Wilhelmy, "Quantifying Trace Elements in Individual Aquatic Protist Cells with a Synchrotron X-ray Fluorescence Microprobe," Analytical Chemistry 75,15 (2003): p. 3806-3816.
11. S. Zelinka, L., S.-C. Gleber, S. Vogt, M. Rodríguez López Gabriela, E. Jakes Joseph, "Threshold for ion movements in wood cell walls below fiber saturation observed by X-ray fluorescence microscopy (XFM)," Holzforschung 69,4 (2015): p. 441-448.
12. J.E. Jakes, C.G. Hunt, D.J. Yelle, L. Lorenz, K. Hirth, S.-C. Gleber, S. Vogt, W. Grigsby, C.R. Frihart, "Synchrotron-based X-ray Fluorescence Microscopy in Conjunction with Nanoindentation to Study Molecular-Scale Interactions of Phenol–Formaldehyde in Wood Cell Walls," ACS applied materials & interfaces 7,12 (2015): p. 6584-6589.
13. R.S. Von Bordwehr, "A history of X-ray absorption fine structure", in: Annales de Physique, Les Editions de Physique, 1989, pp. 377-465.
14. M. Wilke, G.M. Partzsch, R. Bernhardt, D. Lattard, "Determination of the iron oxidation state in basaltic glasses using XANES at the K-edge," Chemical Geology 220,1 (2005): p. 143-161.
15. C. Lamberti, S. Bordiga, F. Bonino, C. Prestipino, G. Berlier, L. Capello, F. D'Acapito, F.L. i Xamena, A. Zecchina, "Determination of the oxidation and coordination state of copper on different Cu-based catalysts by XANES spectroscopy in situ or in operando conditions," Physical Chemistry Chemical Physics 5,20 (2003): p. 4502-4509.
16. K. Xia, F. Weesner, W. Bleam, P. Helmke, P. Bloom, U. Skyllberg, "XANES studies of oxidation states of sulfur in aquatic and soil humic substances," Soil Science Society of America Journal 62,5 (1998): p. 1240-1246.
17. D. Schulze, S. Sutton, S. Bajt, "Determining manganese oxidation state in soils using X-ray absorption near-edge structure (XANES) spectroscopy," Soil Science Society of America Journal 59,6 (1995): p. 1540-1548.
18. Anon, *AWPA P5: Standard for waterborne preservatives*, (American Wood Preservers' Association, Granbury, TX, 2007),
19. Anon, *ICC-ES Evaluation Report ESR-1980. Naturewood and Micropro/Smart Sense pressure treated wood.*, (ICC Evaluation Service, Birmingham, AL, 2013),
20. S. Vogt, "MAPS: A set of software tools for analysis and visualization of 3D X-ray fluorescence data sets," Journal de physique. IV 104,(2003): p. 635-638.
21. B. Ravel, M. Newville, "ATHENA, ARTEMIS, HEPHAESTUS: data analysis for X-ray absorption spectroscopy using IFEFFIT," Journal of synchrotron radiation 12,4 (2005): p. 537-541.